

Supplementary Materials: Inverse energy transfer in three-dimensional quantum vortex flows

P. Z. Stasiak,¹ C.F. Barenghi,¹ A. Baggaley,^{1,2} G. Krstulovic,³ and L. Galantucci⁴

¹School of Mathematics, Statistics and Physics, Newcastle University,
Newcastle upon Tyne, NE1 7RU, United Kingdom

²Department of Mathematics and Statistics, Lancaster University, Lancaster, LA1 4YF, UK

³Université Côte d'Azur, Observatoire de la Côte d'Azur, CNRS, Laboratoire Lagrange,
Boulevard de l'Observatoire CS 34229 - F 06304 NICE Cedex 4, France

⁴Istituto per le Applicazioni del Calcolo "M. Picone" IAC CNR, Via dei Taurini 19, 00185 Roma, Italy

NUMERICAL METHOD

Using Schwarz mesoscopic model [1], vortex lines can be described as space curves $\mathbf{s}(\xi, t)$ of infinitesimal thickness, with a single quantum of circulation $\kappa = h/m_4 = 9.97 \times 10^{-8} \text{ m}^2/\text{s}$, where h is Planck's constant, $m_4 = 6.65 \times 10^{-27} \text{ kg}$ is the mass of one helium atom, ξ is the natural parameterization, arclength, and t is time. These conditions are a good approximation, since the vortex core radius of superfluid ${}^4\text{He}$ ($a_0 = 10^{-10} \text{ m}$) is much smaller than any of the length scales of interest in turbulent flows. The equation of motion is

$$\dot{\mathbf{s}}(\xi, t) = \mathbf{v}_s + \frac{\rho_n}{\rho} [\mathbf{v}_{ns} \cdot \mathbf{s}'] \mathbf{s}' + \beta \mathbf{s}' \times \mathbf{v}_{ns} + \beta' \mathbf{s}' \times [\mathbf{s}' \times \mathbf{v}_{ns}], \quad (1)$$

where $\dot{\mathbf{s}} = \partial \mathbf{s} / \partial t$, $\mathbf{s}' = \partial \mathbf{s} / \partial \xi$ is the unit tangent vector, $\mathbf{v}_{ns} = \mathbf{v}_n - \mathbf{v}_s$, \mathbf{v}_n and \mathbf{v}_s are the normal fluid and superfluid velocities at \mathbf{s} and β, β' are temperature and Reynolds number dependent mutual friction coefficients [2]. The superfluid velocity \mathbf{v}_s at a point \mathbf{x} is determined by the Biot-Savart law

$$\mathbf{v}_s(\mathbf{x}, t) = \frac{\kappa}{4\pi} \oint_{\mathcal{T}} \frac{\mathbf{s}'(\xi, t) \times [\mathbf{x} - \mathbf{s}(\xi, t)]}{|\mathbf{x} - \mathbf{s}(\xi, t)|} d\xi, \quad (2)$$

where \mathcal{T} represents the entire vortex configuration. There is currently a lack of a well-defined theory of vortex reconnections in superfluid helium, like for the Gross-Pitaevskii equation [3–5]. An *ad hoc* vortex reconnection algorithm is employed to resolve the collisions of vortex lines [6].

A *two-way model* is crucial to understand the accurately interpret the back-reaction effect of the normal fluid on the vortex line and vice-versa [7]. We self-consistently evolve the normal fluid \mathbf{v}_n with a modified Navier-Stokes equation

$$\frac{\partial \mathbf{v}_n}{\partial t} + (\mathbf{v}_n \cdot \nabla) \mathbf{v}_n = -\nabla \frac{p}{\rho} + \nu_n \nabla^2 \mathbf{v}_n + \frac{\mathbf{F}_{ns}}{\rho_n}, \quad (3)$$

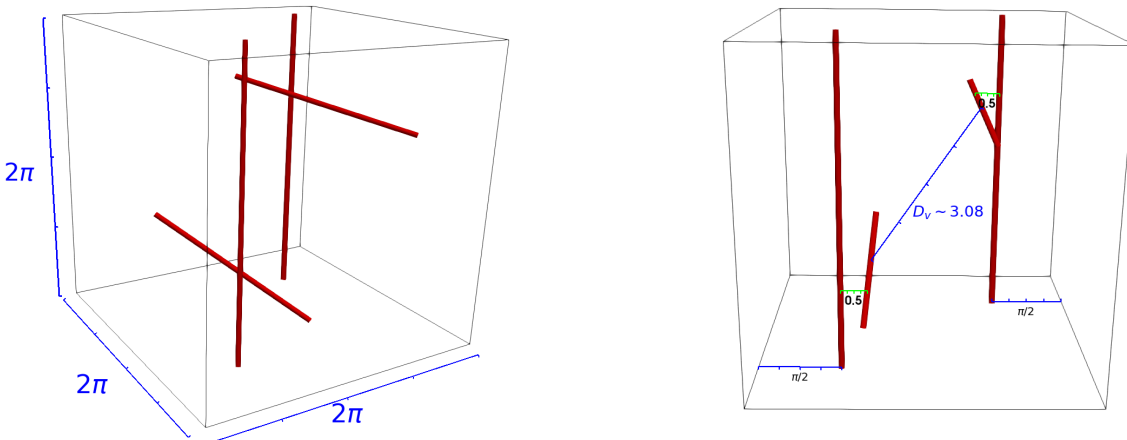


FIG. 1: Schematic diagram of the orthogonal vortex configuration.

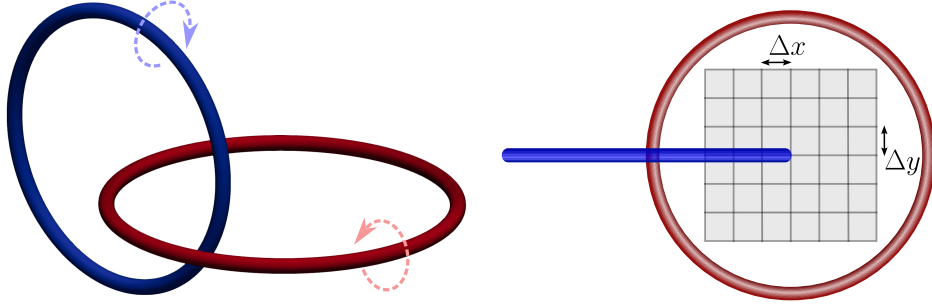


FIG. 2: Schematic diagram of the Hopf link vortex configuration.

$$\mathbf{F}_{ns} = \oint_{\mathcal{T}} \mathbf{f}_{ns} \delta(\mathbf{x} - \mathbf{x}) d\xi, \quad \nabla \cdot \mathbf{v}_n = 0, \quad (4)$$

where $\rho = \rho_n + \rho_s$ is the total density, ρ_n and ρ_s are the normal fluid and superfluid densities, p is the pressure, ν_n is the kinematic viscosity of the normal fluid and \mathbf{f}_{ns} is the local friction per unit length [8]

$$\mathbf{f}_{ns} = -\mathcal{D}\mathbf{s}' \times [\mathbf{s}' \times (\dot{\mathbf{s}} - \mathbf{v}_n)] - \rho_n \kappa \mathbf{s}' \times (\mathbf{v}_n - \dot{\mathbf{s}}), \quad (5)$$

where \mathcal{D} is a coefficient dependent on the vortex Reynolds number and intrinsic properties of the normal fluid. The regularization of the mutual friction force onto the normal fluid grid is physically motivated by the strongly localized injection of vorticity during the momentum exchange of point-like particles and viscous flow in classical fluid dynamics [9, 10]. In short, the localized vorticity induced by the relative motion between the vortex lines and the normal fluid is diffused to discretization of the grid spacing Δx in a time interval ϵ_R . In this way, the delta-forced friction as defined in Eq. 5 is regularized by a Gaussian function, the fundamental solution of the diffusion equation. Further details of the method for classical fluids are contained in [9, 10] and for FOUCAULT in [2].

In this Letter, we report all results using dimensionless units, where the characteristic length scale is $\tilde{\lambda} = D/D_0$, where $D^3 = (1 \times 10^{-3} \text{m})^3$ is the dimensional cube size, $D_0^3 = (2\pi)^3$ is the non-dimensional cubic computational domain. The time scale is given by $\tilde{\tau} = \tilde{\lambda}^2 \nu_n^0 / \nu_n$, where the non-dimensional viscosity ν_n^0 resolves the small scales of the normal fluid. In this work, we consider two vortex configurations - initially orthogonal vortices and Hopf links.

Orthogonal reconnection: The characteristic quantities are $\tilde{\lambda} = 1.59 \times 10^{-4} \text{m}$, $\nu_n^0 = 0.32$ and $\tilde{\tau} = 0.366 \text{s}$ at $T = 1.9K$ and $\tilde{\tau} = 0.485 \text{s}$ at $T = 2.1K$. The vortices are initialized as two pairs of orthogonal vortices, as shown in the schematic of Fig. 1. The separation between vortices in each pair d is set to be $d_v = 0.5$ in dimensionless units, and the shortest distance between pairs is $D_v = \sqrt{(\pi - d_v/2)^2 + \pi^2} \approx 3.08$, so that $d_v \ll D_v$. The Lagrangian discretization of vortex lines is $\Delta\xi = 0.025$ (a total of 1340 discretization points across the 4 vortex lines), using a timestep of $\Delta t_{VF} = 5.56 \times 10^{-6}$. For the normal fluid, a total of $N = 256^3$ mesh points were used, with a timestep of $\Delta t_{NS} = 45\Delta t_{VF}$.

Hopf link: The characteristic quantities are $\tilde{\lambda} = 1.59 \times 10^{-4} \text{m}$, $\nu_n^0 = 0.16$ and $\tilde{\tau} = 0.1836 \text{s}$ at $T = 1.9K$ and $\tilde{\tau} = 0.2439 \text{s}$ at $T = 2.1K$. Vortices are initialized as shown in Fig. 2, where the blue vortex ring is chosen at an initial offset $n_x \Delta x$ and $n_y \Delta y$ where $n_x, n_y \in \{-3, \dots, 3\}$ and $\Delta x = \Delta y = 0.125$ in units of the code. This gives a total of 49 individual reconnections for each temperature. Both of the rings have radius $R \approx 1$ also in units of the code. Furthermore, each reconnection is supplemented with a normal fluid ring around the superfluid vortex ring, which is generated by superimposing a normal fluid ring generated by a propagating ring of the same radius. In this way, we eliminate a transient phase of generating normal fluid structures. The Lagrangian discretization of the vortex lines is $\Delta\xi = 0.025$ (a total of 668 discretization points across both of the rings), using a timestep of $\Delta t_{VF} = 1.25 \times 10^{-5}$. For the normal fluid, a total of $N = 256^3$ mesh points were used, with a timestep of $\Delta t_{NS} = 40\Delta t_{VF}$.

HELICAL DECOMPOSITION OF THE FLOW FOR HOPF LINK SIMULATIONS

In the main text we presented the inverse energy transfer mechanism in the context of an initially orthogonal pair of vortices, separated by an initial distance $d = 0.5$ in units of the code. The reconnection of orthogonal filaments is

the most violent type of vortex reconnections (the separation is much faster than the approach), and therefore shows the most clear manifestation of a chiral imbalance and hence an inverse energy transfer. However, the inverse energy transfer due to the reconnection of superfluid vortices is not limited to this geometry specifically, and will hold in general where the injection of helicity in the flow produces a chiral imbalance. To illustrate this point, we perform the same analysis as for the orthogonal reconnections on a series of Hopf link reconnections, which are shown schematically in Fig. 2. We sample two reconnections for each temperature to use for the analysis, which represent the extrema the pre/post reconnection characteristics. The minimum distance of two reconnecting filaments is well-known to scale with a 1/2 power law [11]

$$\delta^\pm = A^\pm |t - t_R|^{1/2}, \quad (6)$$

where the A represents a dimensionless prefactor and \pm is used to distinguish between the pre- and post-reconnection quantities. The ratio of $A_r = A^+/A^-$ has been shown using Gross-Pitaveskii models to be an important quantity that determines the geometric properties of vortex reconnections, such as the reconnection angle [3]. We define A_{min} and A_{max} to represent two Hopf link reconnections which represent the smallest and largest differences between the approach and separation speeds of reconnecting filaments. In other words,

$$A_{min} = \min\{A^+/A^-\} \quad A_{max} = \max\{A^+/A^-\}. \quad (7)$$

Therefore, A_{min} is related to the reconnection event where the separation speed is similar to the approach speed and $A^+/A^- \gtrsim 1$, while A_{max} is related to other extreme, where the separation speed is much greater than approach so

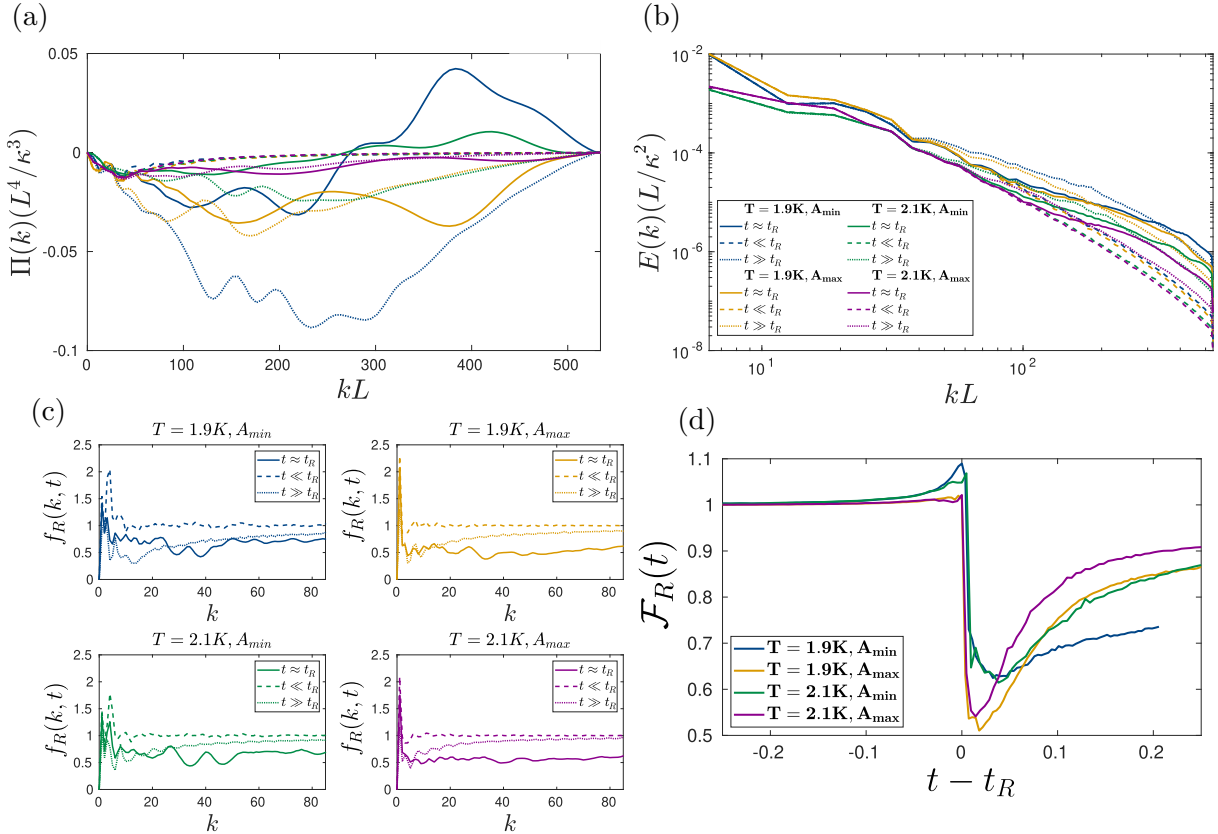


FIG. 3: (a) The scaled spectral kinetic energy flux $\Pi(k)$ for a sample of 2 Hopf link simulations across two temperatures $T = 1.9\text{K}$ and $T = 2.1\text{K}$. The colour scheme of the lines and the linestyles is the same as for (b). Solid lines represent the time around reconnection, while dashed and dotted lines represent times much smaller and greater than the reconnection event respectively. (b) The scaled kinetic energy spectrum for the same 4 Hopf link simulations. (c) The spectrum of the ratio of the squared projected mutual friction helical modes $f_R(k,t)$, separated by temperature T and the ratio of the dimensionless parameters A^+/A^- . (d) Time evolution of the squared projected helical modes $\mathcal{F}_R(t)$.

that $A^+/A^- \gg 1$. The results of the analysis is shown in Fig. 3, which shows a definitive chiral imbalance of mutual friction helical modes due to the reconnection event. We define the spectral ratio of the squared projected mutual friction helical modes f_R by

$$f_R(k, t^*) = \frac{|f^+(k, t^*)|^2}{|f^-(k, t^*)|^2}, \quad (8)$$

given a fixed t^* , and evolution of this ratio of modes by \mathcal{F}_R where

$$\mathcal{F}_R(t) = \frac{\int dk |f^+(k, t)|^2}{\int dk |f^-(k, t)|^2}. \quad (9)$$

-
- [1] KW. Schwarz, Three-dimensional vortex dynamics in superfluid ${}^4\text{He}$, Phys. Rev. B **38**, 2398 (1988).
 - [2] L. Galantucci, A. W. Baggaley, C. F. Barenghi, and G. Krstulovic, A new self-consistent approach of quantum turbulence in superfluid helium, Eur. Phys. J. Plus **135**, 547 (2020).
 - [3] A. Villois, D. Proment, and G. Krstulovic, Irreversible Dynamics of Vortex Reconstructions in Quantum Fluids, Phys. Rev. Lett. **125**, 164501 (2020).
 - [4] A. Villois, D. Proment, and G. Krstulovic, Universal and nonuniversal aspects of vortex reconstructions in superfluids, Phys. Rev. Fluids **2**, 044701 (2017).
 - [5] D. Proment and G. Krstulovic, Matching theory to characterize sound emission during vortex reconnection in quantum fluids, Phys. Rev. Fluids **5**, 104701 (2020).
 - [6] A. W. Baggaley, The sensitivity of the vortex filament method to different reconnection models, J. Low Temp. Phys. **168**, 18 (2012).
 - [7] P. Z. Stasiak, A. W. Baggaley, G. Krstulovic, C. F. Barenghi, and L. Galantucci, Cross-Component Energy Transfer in Superfluid Helium-4, J Low Temp Phys 10.1007/s10909-023-03042-5 (2024).
 - [8] L. Galantucci, M. Sciacca, and CF. Barenghi, Coupled normal fluid and superfluid profiles of turbulent helium II in channels, Phys Rev B **92**, 174530 (2015).
 - [9] P. Gualtieri, F. Picano, G. Sardina, and C. M. Casciola, Exact regularized point particle method for multiphase flows in the two-way coupling regime, Journal of Fluid Mechanics **773**, 520 (2015).
 - [10] P. Gualtieri, F. Battista, and C. M. Casciola, Turbulence modulation in heavy-loaded suspensions of tiny particles, Physical Review Fluids **2**, 034304 (2017).
 - [11] P. Z. Stasiak, Y. Xing, Y. Alihosseini, C. F. Barenghi, A. Baggaley, W. Guo, L. Galantucci, and G. Krstulovic, Experimental and theoretical evidence of universality in superfluid vortex reconstructions, Proc. Nat. Acad. of Sci. **122**, e2426064122 (2025).